

DRIVE-BY STRUCTURAL HEALTH MONITORING OF RAILWAY BRIDGES USING TRAIN-MOUNTED ACCELEROMETERS

Cathal Bowe¹, Paraic Quirke^{1,2}, Daniel Cantero³, and Eugene J. OBrien^{2,3}

¹ Iarnród Éireann - Irish Rail
Technical Department, Engineering & New Works, Inchicore, Dublin 8, Ireland.
e-mail: cathal.bowe@irishrail.ie; paraic.quirke@irishrail.ie

² School of Civil, Structural and Environmental Engineering and Earth Institute
University College Dublin, Dublin 4, Ireland.
eugene.obrien@ucd.ie

³ Roughan O'Donovan Innovative Solutions
Arena House, Arena Road, Sandyford, Dublin 18, Ireland.
daniel.cantero@rod.ie

Keywords: Railway, Bridge, Structural Health Monitoring, Drive-by, Dynamics, Maintenance.

Abstract. *Bridge damage can be detected by observing changes in its spectral properties. In its infancy, bridge health monitoring involved monitoring physical properties via direct instrumentation, i.e. sensors attached to the bridge. In recent years many authors have investigated the ability of indirect methods to assess the structural health of bridges, i.e. the vehicles traversing the bridges are fitted with sensors. This has the potential of reducing monitoring costs as the vehicle may be used to monitor many bridges on the network. Most of the investigation in this relatively new field of study has been on road bridges and road vehicles. A method is proposed in this paper for the detection of the bridge damage through an analysis of vehicle accelerations resulting from the train/track/bridge dynamic interaction. In a train/track/bridge interaction there are additional complications which do not exist on road bridges. The signal generated by the train as it traverses the bridge is normally short in duration. Studies on railway bridges are complicated by the addition of rails, sleepers and sometimes ballast between the tracks and the bridge deck. However, the weight of the train relative to the bridge is considerably larger than previous studies using road vehicles and this will excite the bridge to a higher degree.*

Numerical validation of the drive-by concept is achieved by using a 2-dimensional dynamic vehicle model with 10 degrees of freedom. The finite element interaction model is implemented in MATLAB. The track is modelled as a continuous beam, supported at 0.545m centres on three layers of springs and masses representing sleepers, and ballast lying on a simply supported bridge beam. This paper reports the results of the numerical simulations and the plans that are underway to test the concept in field trials.

1 INTRODUCTION

At present most condition monitoring of bridges on rail networks is carried out by periodic visual inspections and non-destructive testing. This monitoring method is time consuming, prone to human error and as such can be unreliable and inconsistent in its findings. Direct instrumentation of bridges, whereby sensors are attached to the bridge, can be used to detect changes in the spectral properties of the structure and infer damage. This method of structural health monitoring is widely documented in the literature [1]. More recently, indirect methods of assessing the structural health of bridges, whereby the measured response of a vehicle crossing the bridge is analysed to detect damage, have gained increased interest in research projects due to the cost saving potential they offer [2]–[4].

The concept, similar to a track damage detection algorithm presented by Cantero and Basu [5], involves using an instrumented vehicle to regularly record geo-located vehicle acceleration responses, establishing a baseline response to a bridge crossing event. The monitoring method makes comparisons to the baseline to detect large differences which could indicate possible structural damage.

For this study it is proposed to analyse the acceleration response of railway vehicles using a continuous wavelet transform, comparing the response to a baseline, or healthy, analysis in order to detect damage in a bridge. The continuous wavelet transform is a time–frequency analysis that provides more detailed information about non-stationary signals which traditional Fourier analysis miss. It is applied to various fields including civil, mechanical and aerospace engineering, especially for damage detection and structural health monitoring (SHM) [6]. Wavelet analysis has advantages over traditional Fourier transform methods in that frequency information is provided while retaining the corresponding time information. The wavelet transform can analyse smaller portions of larger signals and return the frequency information for that portion. This property of the transform means it has the potential, not only to detect damage, but also to locate it. The wavelet transform was developed by Daubechies [7]. Definitions of the wavelet transform and descriptions of the most common wavelets are published in her work. The wavelets most commonly used in structural health monitoring are investigated by Reda-Taha *et al.*, [8] who find that some wavelets perform better in certain situations. A number of authors use the ‘Mexican Hat’ wavelet in structural health monitoring and bridge damage investigations [9], [10], and is therefore adopted as part of this study.

Zhu and Law [9] use wavelet analysis to detect an irregularity in a beam using its displacement response. Hester *et al.* [10] build on that work by applying the wavelet transform to bridge deck acceleration responses in order to increase the level of accuracy required when assessing vehicle bridge interactions. Hester *et al.* assess the wavelet energy of a signal by squaring the wavelet coefficients over incremental time intervals.

Wimmer *et al.* [11] use experimental data from strain sensors to measure the excitation of a flat steel plate to detect damage in welds along the edge of the plate. This is achieved by comparison of the wavelet transform of the strain data to a baseline state and examining the maximum difference in wavelet transform coefficients.

In this study, the acceleration response of a railway vehicle is generated using a validated finite-element vehicle-bridge interaction model called the Train-Track-Bridge (TTB) model developed by Cantero *et al.* [12]. The model generates acceleration responses at any degree of freedom in the structure or vehicle. Damage is simulated in the bridge structure by reducing the stiffness of affected bridge elements. Acceleration outputs from the TTB model provide the inputs for the wavelet-based damage detection algorithm. Wavelet transforms for vehicle acceleration responses measured for different levels of damage are compared to investigate if damage can be detected and located.

This paper is divided into the following sections. Firstly, the Train-Track-Bridge model used in the investigation is described. This is followed by a brief section describing the wavelet tool and methodology. Results are presented for a range of damage levels, locations and signal noise. Finally, an overview of the results and suggestions for further research are presented.

2 MODEL DESCRIPTION

The Train-Track-Bridge (TTB) model is presented in this section. The vehicle model, track model and bridge model are all described separately before the coupling of the model is briefly described.

2.1 Vehicle Model

The vehicle model used in this study is shown in Figure 1. The vehicle is modelled as a ‘half-car’ consisting of 10 Degrees Of Freedom (DOF) including 4 wheels (vertical displacements only), 2 bogies (vertical displacement and rotation about the centre of gravity on each bogie) and the main body (vertical displacement and rotation about the centre of gravity of the main body). The wheels are represented as masses (m_{w1} , m_{w2} , m_{w3} , m_{w4}). The bogies are modelled as rigid bars with mass (m_{b1} , m_{b2}) and moment of inertia (I_{b1} , I_{b2}), while the main body of the vehicle is modelled as a rigid bar with mass (m_v) and moment of inertia (I_v). The wheels are connected to the bogies by means of primary suspension systems consisting of springs (k_p) and viscous dampers (c_p) in parallel. Similarly, the bogies are connected to the main body by means of a secondary suspension system consisting of a spring (k_s) and a viscous damper (c_s) in parallel. Assuming small rotations, we can adopt a linearized system of equations of motion. Vehicle properties are gathered from the literature [13] and are listed in Table 1.

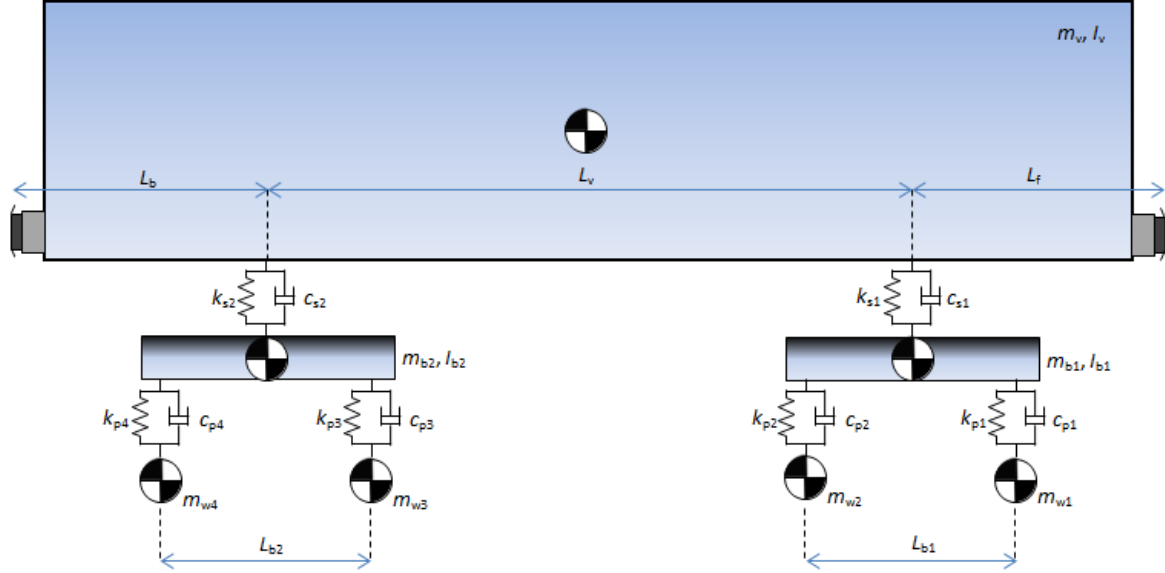


Figure 1: Sketch of vehicle model

Property	Symbol	Value	Unit
Mass of wheel	$m_{w1}, m_{w2}, m_{w3}, m_{w4}$	1843.5	kg
Mass of bogie	m_{b1}, m_{b2}	5630.8	kg
Mass of main body	m_v	59364.2	kg
Moment of Inertia of bogie	I_{b1}, I_{b2}	9487	kg.m ²
Moment of Inertia of main body	I_v	1.723×10^6	kg.m ²
Stiffness of Primary Suspension	$k_{p1}, k_{p2}, k_{p3}, k_{p4}$	4.7992×10^6	N/m
Stiffness of Secondary Suspension	k_{s1}, k_{s2}	1.7716×10^6	N/m
Damping of Primary Suspension	$c_{p1}, c_{p2}, c_{p3}, c_{p4}$	60×10^3	Ns/m
Damping of Secondary Suspension	c_{s1}, c_{s2}	90×10^3	Ns/m
Distance between bogies	L_v	11.46	m
Additional distance (front and back)	L_b, L_f	3	m
Distance between axles	L_{b1}, L_{b2}	3	m

Table 1: Properties of the vehicle – Chinese Star – Power Car.

2.2 Track Model

The track is modelled as a beam supported on a three-layer sprung mass system representing a sleeper, pad and ballast support system as shown in Figure 2. This three-layer system is the structure recommended by the UIC for assessing rail bridges due to dynamic interaction between the train, track and bridge [14]. Track supports are spaced at a regular interval L_s , representing the spacing between the sleepers. The rail is modelled as a finite element Euler-Bernoulli beam with two beam elements per sleeper spacing. Each track element has 2 nodes with 2 DOF at each node. Properties of track structures vary significantly throughout the literature. Values used in this study are taken from Zhai *et al.*[15] and are shown in Table 2. Note that properties marked with an asterisk (*) in the table are for single rail only and are doubled in order to include both rails in the planar TTb model. Ballast is omitted over the bridge where sleepers are fixed directly to the beam. Vibrations are dissipated through sleeper-beam pads, the properties of which are shown in Table 2.

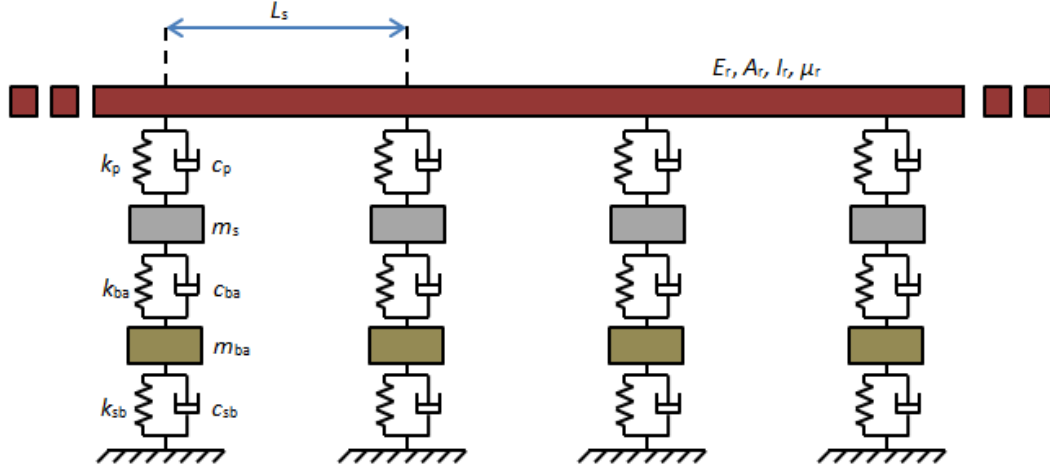


Figure 2: Sketch of track model

Property	Symbol	Value	Unit
Elastic modulus of rail	E_r	2.059×10^{11}	N/m ²
Rail cross-sectional area	A_r	7.69×10^{-3}	m ²
Rail second moment of area	I_r	$*3.217 \times 10^{-5}$	m ⁴
Rail mass per unit length	μ_r	$*60.64$	kg/m
Rail Pad stiffness	k_p	6.5×10^7	N/m
Rail Pad damping	c_p	7.5×10^4	Ns/m
Sleeper mass (half)	m_s	$*125.5$	kg
Sleeper spacing	L_s	0.545	m
Ballast stiffness	k_{ba}	137.75×10^6	N/m
Ballast damping	c_{ba}	5.88×10^4	Ns/m
Ballast mass	m_{ba}	531.4	kg
Sub-ballast stiffness	k_{sb}	77.5×10^6	N/m
Sub-ballast damping	c_{sb}	3.115×10^4	Ns/m
Beam-sleeper pad stiffness	k_{bs}	77.5×10^6	N/m
Beam-sleeper pad damping	c_{bs}	90×10^3	Ns/m

Table 2: Properties of the track

2.3 Bridge Model

The bridge used in this study is shown in Figure 3. The bridge is modelled as a simply supported finite element beam with properties listed in Table 3. For the purposes of symmetry the beam element length is equal to the track model element length, i.e. half the sleeper spacing, resulting in a total of 74 elements in the beam. Each beam element has 2 nodes with 2 DOF at each node. Properties of the concrete beam have been taken from the literature [16].

The theory behind global damage detection methods is that damage changes the stiffness, mass or damping properties of a structure, altering its dynamic response. Damage in the beam is modelled simply as a percentage loss of sectional depth in selected elements producing a reduction in the elemental stiffness of the affected elements in the beam.

Rayleigh damping is used in the model to simulate energy dissipation in the beam response.

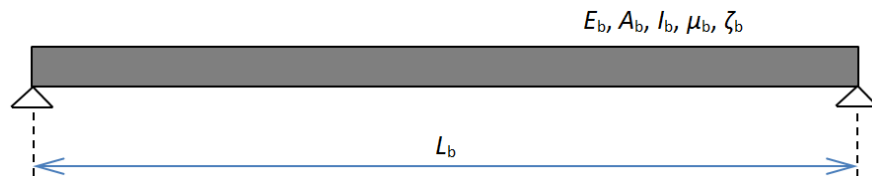


Figure 3: Sketch of beam model

Property	Symbol	Value	Unit
Length	L_b	20	m
Elastic modulus	E_b	25×10^9	N/m ²
Second moment of area	I_b	1.46	m ⁴
Damping ratio	ζ_b	1	%
Cross-sectional area	A_b	1	m ²
Mass per unit length	μ_b	17777	kg/m

Table 3: Properties of the beam

2.4 Coupled Model

The vehicle, track and beam subsystems are combined together to form the TTB model. The model can be visualised in Figure 4. A static analysis is carried out before a dynamic analysis is initiated. Furthermore, a bridge approach distance of 10 m from the leading wheel to the left hand bridge support, is incorporated into the model to allow the vehicle achieve dynamic equilibrium before the first wheel enters the bridge. A section of track is included after the bridge to allow the vehicle to fully exit the bridge and for free vibration of the bridge to take place after the vehicle has passed.

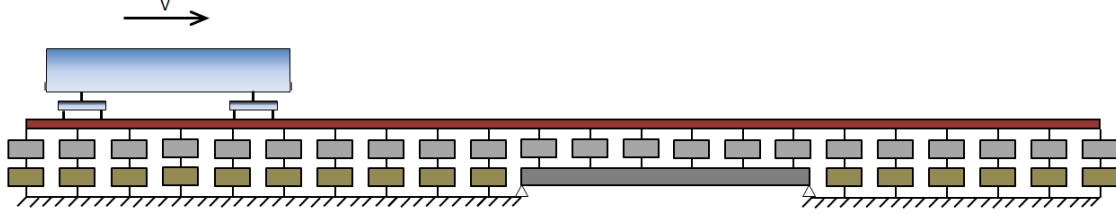


Figure 4: Sketch of TTB model

The vehicle track and beam subsystems can each be defined by a set of second order differential equations that can be represented in matrix format as:

$$M_x \ddot{u}_x + C_x \dot{u}_x + K_x u_x = F_x \quad (1)$$

where M , C and K are the mass, damping and stiffness matrices of the subsystem respectively. The subscript 'x' denotes which subsystem the matrix refers to and may be substituted by V, T, and B to denote the vehicle, track and bridge subsystems respectively. F is the external force vector while \ddot{u} , \dot{u} and u are the vectors of accelerations, velocities and displacements respectively. The coupling of the subsystems is expressed mathematically with additional off-diagonal block matrices as shown in Eqn (2).

$$\begin{pmatrix} M_V & 0 & 0 \\ 0 & M_T & 0 \\ 0 & 0 & M_B \end{pmatrix} \begin{Bmatrix} \ddot{u}_V \\ \ddot{u}_T \\ \ddot{u}_B \end{Bmatrix} + \begin{pmatrix} C_V & C_{V,T} & 0 \\ C_{T,V} & C_T & C_{T,B} \\ 0 & C_{B,T} & C_B \end{pmatrix} \begin{Bmatrix} \dot{u}_V \\ \dot{u}_T \\ \dot{u}_B \end{Bmatrix} + \begin{pmatrix} K_V & K_{V,T} & 0 \\ K_{T,V} & K_T & K_{T,B} \\ 0 & K_{B,T} & K_B \end{pmatrix} \begin{Bmatrix} u_V \\ u_T \\ u_B \end{Bmatrix} = \begin{Bmatrix} F_V \\ F_T \\ F_B \end{Bmatrix} \quad (2)$$

The vehicle and track/bridge model are coupled together via the wheel/rail interaction, i.e. the DOF's of the wheels and the DOF's of the rail are combined. The coupling terms in the coupled matrices need to be updated at each time step. The vehicle wheels do not always act at the nodes of the rail and the vehicle's contribution to the coupled terms needs to be distributed to the DOF's of the rail using Hermitian shape functions. This method of distribution is well documented in the literature [17].

The equations of motion are solved using a numerical integration scheme. The Newmark- β method is employed in this study [18]. The TTB model was implemented in Matlab.

3 WAVELET ANALYSIS

A wavelet is a waveform of limited duration with an average value of zero.

$$\int_{-\infty}^{+\infty} \psi(x) dx = 0 \quad (3)$$

where $\psi(x)$ is the base or mother wavelet. The base wavelet can be scaled and translated to create a range of analysing wavelets:

$$\psi(x)_{\bar{x},s} = \frac{1}{\sqrt{s}} \psi\left(\frac{x-\bar{x}}{s}\right) \quad (4)$$

where s is the scaling factor and \bar{x} is the translation parameter. The base wavelet can be a real or complex function; however only real wavelets are used in this study. The continuous wavelet transform of a function, or in this study, a continuous acceleration signal, $y(x)$, is given by the following equation:

$$Y(x,s)_w = \int_{-\infty}^{+\infty} y(x) \frac{1}{\sqrt{s}} \psi\left(\frac{x-\bar{x}}{s}\right) dx \quad (5)$$

where $Y(x,s)_w$ refers to the transformed quantity, or coefficient, of $y(x)$ using the wavelet, $\psi(x)_{\bar{x},s}$.

In a wavelet transform the base wavelet is compared to a portion of the signal being analysed and its coefficient is calculated. The wavelet coefficient is a measure of how closely the base wavelet matches the function in the area of interest. The wavelet is translated along the entire signal resulting in a series of wavelet coefficients in time. The wavelet is then scaled, or stretched, and the process is repeated until the signal has been analysed by all scales in a specified range. The result of the analysis is a 3-dimensional surface or 2-dimensional contour plot in which wavelet coefficients, scales and time can be represented [8].

The scale axis of the plot can be related to a pseudo frequency [10]. A large scaling factor implies a stretched base wavelet that detects low frequency content in the signal. A low scaling factor detects high frequency content in the signal. There exists a relationship between the scale of the base wavelet and a pseudo frequency given by the following equation:

$$F_s = \frac{F_c}{s\Delta} \quad (6)$$

where F_s is the pseudo frequency corresponding to scale, s , in Hz, F_c is the centre frequency of the wavelet in Hz and Δ is the sampling period of the signal being analysed.

In this study the TTB model is used to simulate the passage of a train across a finite element track model featuring a bridge beam as described in Section 2. The acceleration response of the front bogie on the vehicle is chosen as the function analysed in the wavelet transform. Two simulations are carried out to generate a ‘healthy’ acceleration response, $y_h(x)$ and a ‘damaged’ response, $y_d(x)$. Wavelet transforms are carried out on both signals independently using the same base wavelet and scale. The difference between the wavelet coefficients for the ‘healthy’ response and ‘damaged’ response is given by the equation:

$$Y(x,s)_w = Y_h(x,s)_w - Y_d(x,s)_w \quad (7)$$

where $Y_h(x,s)_w$ represents the wavelet coefficients calculated for the ‘healthy’ response $y_h(x)$, and $Y_d(x,s)_w$ represents the wavelet coefficients calculated for the ‘damaged’ response $y_d(x)$. With all other parameters being equal, the difference in the wavelet coefficients will return the magnitude and location of the damage in the beam.

4 RESULTS AND DISCUSSION

In the first simulation, the vehicle is simulated traversing the model with a smooth rail profile and no bridge damage at a constant velocity of 120 km/hr, producing a healthy acceleration response. For the second simulation, damage is introduced into the bridge in elements 22 and 23 (out of a total of 74 elements), and the same vehicle is simulated crossing the model

from the same starting point at the same velocity. A comparison of the wavelet transform produced is shown in Figure 5. It is shown that damage is located where the maximum difference between the healthy and damaged wavelet coefficients occurs.

It is found that scales between 10 and 50 (corresponding to pseudo-frequencies of 20 Hz – 2 Hz) are most successful in finding the damage and damage location using the Mexican hat wavelet for this particular model. The first mode of vibration of the healthy bridge (5.535Hz) is found within the corresponding frequency range. Damage causes a change to the natural frequencies of the bridge which manifests itself in the vehicle response thereby allowing the detection of the damage from the vehicle response.

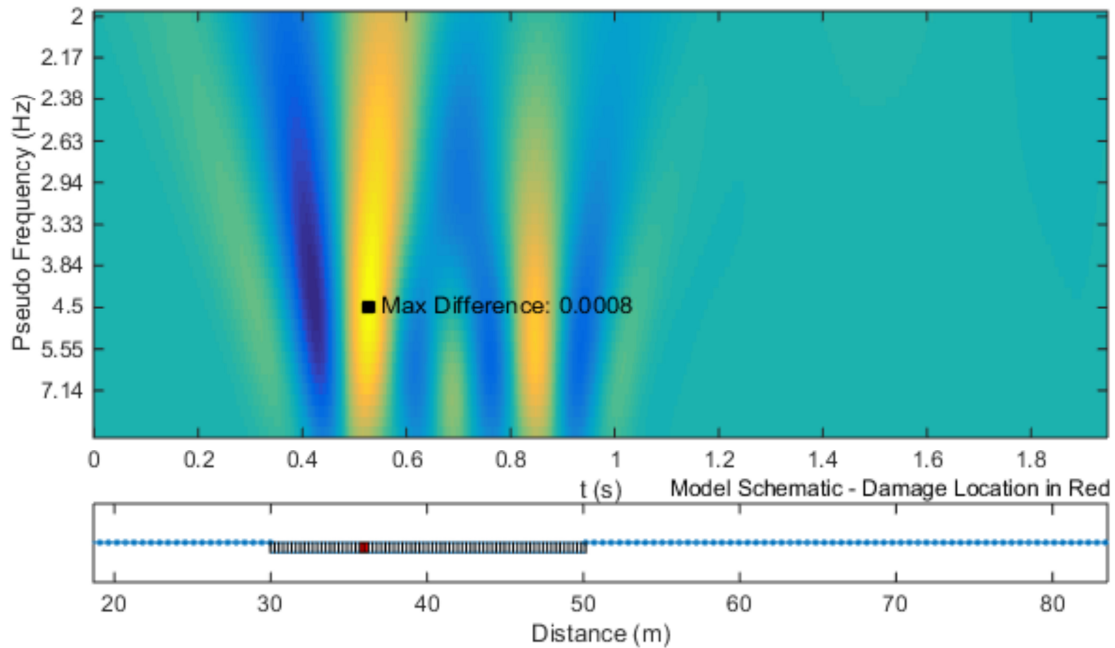


Figure 5: Wavelet contour plot showing difference in Wavelet Coefficients for Bogie1 Accelerations - 0% Noise - 10% Damage

For the next simulation, damage is increased by 10% to 20% in the same beam elements. All other parameters are unchanged. Again, the wavelet transform for the acceleration responses are compared. The differences in the wavelet transform coefficients are shown in Figure 6. As before, the presence of damage, and its location, are determined. By comparison to Figure 5 an estimation of the relative magnitude of the damage can also be made. In Figure 5 the magnitude of the maximum difference was 0.0008 for 10% damage. For 20% damage it is found that the maximum difference is just over twice that (0.0018).

To determine if a relationship exists between the difference in wavelet coefficients and damage level, a number of simulations were carried out and the maximum difference between wavelet functions determined for increasing damage level. Figure 7 shows that the maximum difference between wavelet coefficients increases with damage level suggesting that the level of damage can be estimated using this approach.

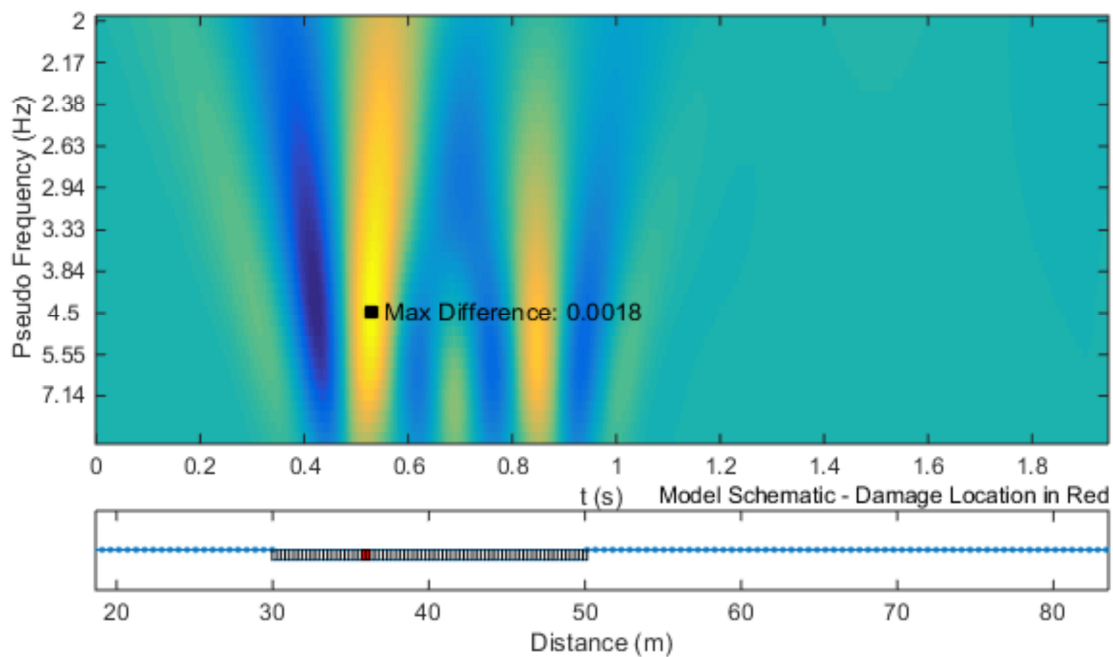


Figure 6: Wavelet Scalogram showing difference in Wavelet Transform Coefficients for Bogie1 Accelerations - 0% Noise - 20% Damage

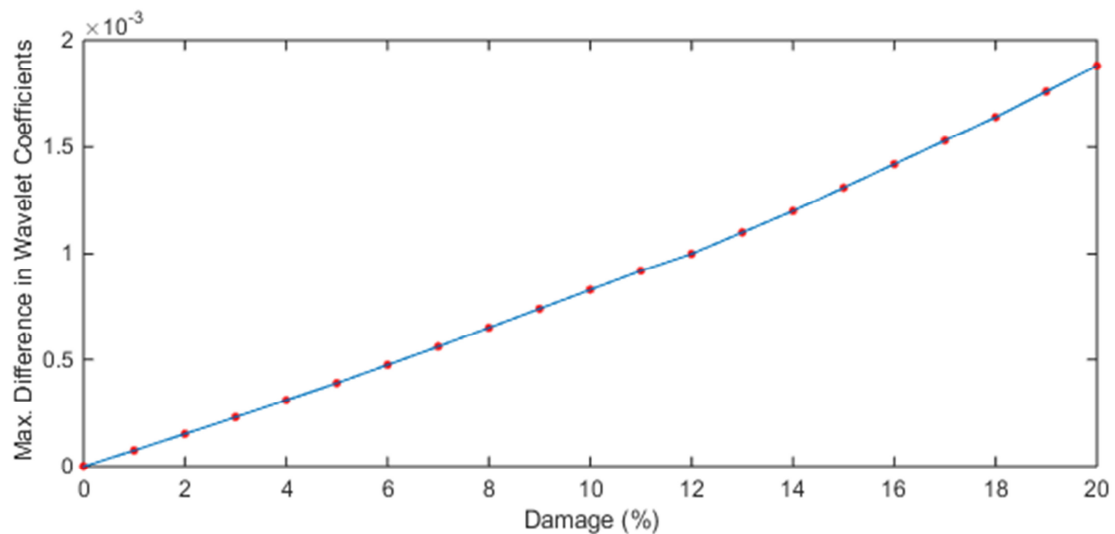


Figure 7: Difference in Wavelet Transform Coefficients vs. Damage

To test the algorithm further, additive white noise related to the signal is introduced to both healthy and damaged signals before wavelet analyses are carried out. Wavelet transforms carried out for both acceleration responses with 1% noise are compared and the differences between the wavelet transform coefficients are shown in Figure 8. As before, the presence of damage, and its location are determined even in the presence of noise. From running multiple simulations for a range of damage levels it is found that damage levels below 5% become generally undetectable in the presence of 1% noise while only damage levels of 8% and above

are detectable when 2% noise is added to the signals. It is found that the addition of noise also reduces the reliability of the damage location capabilities of the algorithm.

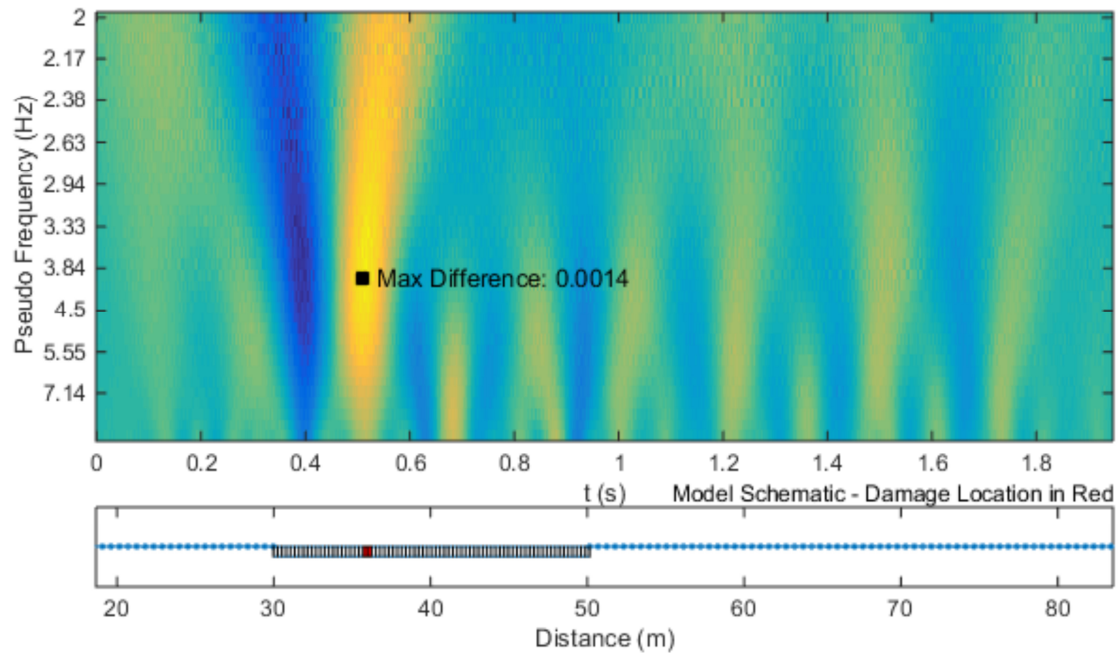


Figure 8: Wavelet contour plot showing difference in Wavelet Transform Coefficients for Bogie1 Accelerations - 1% Noise - 10% Damage

5 CONCLUSIONS

A methodology has been presented whereby damage in a bridge can be detected using instrumentation fitted to a traversing vehicle. A wavelet transform-based damage identification and location technique has been found to be simple, efficient, and independent of damage magnitude and location with an acceptable tolerance to signal noise. The basis of the technique is the comparison of vehicle acceleration response while crossing a damaged bridge to a healthy baseline response. Variations in the acceleration response due to variations in the global properties of the bridge resulting from the bridge damage can be detected as a difference in the resulting wavelet plots.

The authors are in the process of acquiring accelerometers to attach to an Irish Rail train vehicle so that the actual acceleration responses of a vehicle can be obtained while it traverses a section of track featuring a bridge. It is planned to acquire the data at regular time intervals in order to make comparative studies into the structural health of the bridge. A potential challenge with the application of this methodology for structural health monitoring of rail bridges using acquired data is the fact that acceleration responses of vehicles can be influenced by many other factors. Obtaining comparable signals may prove difficult.

6 ACKNOWLEDGEMENTS

The research presented in this paper was carried out as part of the Marie Curie Initial Training Network (ITN) action FP7-PEOPLE-2013-ITN. The project has received funding from the European Union's Seventh Framework Programme for research, technological development and demonstration under grant agreement number 607524. The authors are thankful for the support.

REFERENCES

- [1] P. C. Chang, A. Flatau, and S. C. Liu, Review Paper : Health Monitoring of Civil Infrastructure, *Structural Health Monitoring*, vol. 2, no. 3, pp. 257–267, 2003.
- [2] P. J. McGetrick, A. González, and E. J. Obrien, Theoretical investigation of the use of a moving vehicle to identify bridge dynamic parameters, *Insight - Non-Destructive Testing and Condition Monitoring*, vol. 51, no. 8, pp. 433–438, Aug. 2009.
- [3] J. Keenahan, P. J. McGetrick, A. González, and E. J. Obrien, Using Instrumented Vehicles to detect damage in bridges, in *15th International Conference on Experimental Mechanics, Porto, Portugal, 22-27 July 2012, Paper No. 2934.*, 2012, vol. 1, pp. 07–22.
- [4] Y. B. Yang and C. W. Lin, Vehicle–bridge interaction dynamics and potential applications, *Journal of Sound and Vibration*, vol. 284, no. 1–2, pp. 205–226, Jun. 2005.
- [5] D. Cantero and B. Basu, Railway infrastructure damage detection using wavelet transformed acceleration response of traversing vehicle, *Structural Control and Health Monitoring*, p. a, 2014.
- [6] H. Kim and H. Melhem, Damage detection of structures by wavelet analysis, *Engineering Structures*, vol. 26, no. 3, pp. 347–362, Feb. 2004.
- [7] I. Daubechies, Ten Lectures on Wavelets, in *CBMS Conference Series 61, SIAM, Philadelphia*, 1992.
- [8] M. M. Reda-Taha, A. Noureldin, J. L. Lucero, and T. J. Baca, Wavelet Transform for Structural Health Monitoring : A Compendium of Uses and Features, *Structural Health Monitoring*, vol. 5, no. 3, pp. 267–295, 2006.
- [9] X. Q. Zhu and S. S. Law, Wavelet-based crack identification of bridge beam from operational deflection time history, *International Journal of Solids and Structures*, vol. 43, no. 7–8, pp. 2299–2317, Apr. 2006.
- [10] D. Hester and A. González, A wavelet-based damage detection algorithm based on bridge acceleration response to a vehicle, *Mechanical Systems and Signal Processing*, vol. 28, pp. 145–166, Apr. 2012.
- [11] S. A. Wimmer and V. G. De Giorgi, A wavelet based algorithm for detecting damage, in Chang, F-K. (ed.), *Proceedings of 4th Int. Workshop on Structural Health Monitoring, Stanford, CA, USA.*, 2003, pp. 395–402.
- [12] D. Cantero, T. Arvidsson, E. J. Obrien, and R. Karoumi, Train-track-bridge dynamic model, validation and review of parameters., *Submitted for publication*, 2014.

- [13] W. Zhai, K. Wang, and C. Cai, Fundamentals of vehicle-track coupled dynamics, *Vehicle System Dynamics: International Journal of Vehicle Mechanics and Mobility*, vol. 47, no. 11, pp. 1349–1376, 2009.
- [14] International Union of Railways. Design requirements for rail-bridges based on phenomena between train, track and bridge, UIC 776-2R. 2009.
- [15] W. M. Zhai, K. Y. Wang, and J. H. Lin, Modelling and experiment of railway ballast vibrations, *Journal of Sound and Vibration*, vol. 270, no. 4–5, pp. 673–683, Mar. 2004.
- [16] S. Rashid, Parametric study of bridge response to high speed trains, 2011.
- [17] P. Lou, Finite element analysis for train–track–bridge interaction system, *Archive of Applied Mechanics*, vol. 77, no. 10, pp. 707–728, Mar. 2007.
- [18] X. Lei and N.-A. Noda, Analyses of dynamic response of vehicle and track coupling system with random irregularity of track vertical profile, *Journal of Sound and Vibration*, vol. 258, no. 1, pp. 147–165, 2002.